Supporting Information

Stepwise Carbon Coated Submicron Silicon Dioxide Anode for Long Life Lithium Ion Batteries

Mengqi Man[a], Yong Guo[a], Tianran Hu[a], Ying Sun*[a,b], Aikai Yang*[c], Xiqing Chen[d], Xingchao Wang*[a]

[a]State Key Laboratory of Chemistry and Utilization of Carbon Based Energy Resources; Institute of Applied Chemistry, College of Chemistry, Xinjiang University, Urumqi, 830017

[b]Xinjiang Autonomous Region Quality Basic Development Research Institute, Urumqi, 830002

[c]Shanghai Ceramic New Materials Co., Ltd, Shanghai 200131, China

[d]Xinjiang Jingshuo new materials CO., LTD. Ganquanbao Economic and Technological Development Zone, 830009

E-mail: xcwang@xju.edu.cn; ichemabc@126.com; aikaiyang@gmail.com

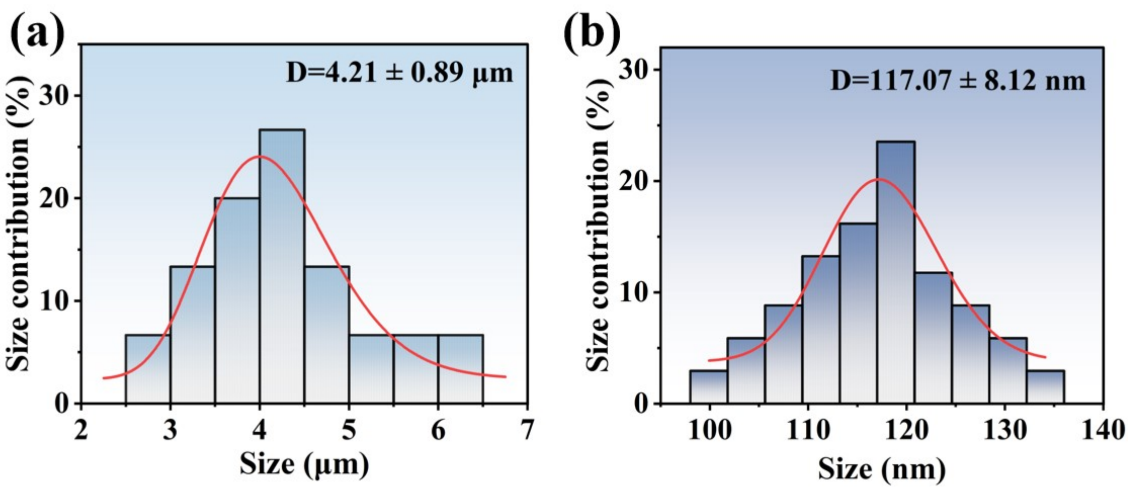

Figure S1. Particle size distributions of (a) D-SiO and (b) SiO-20.

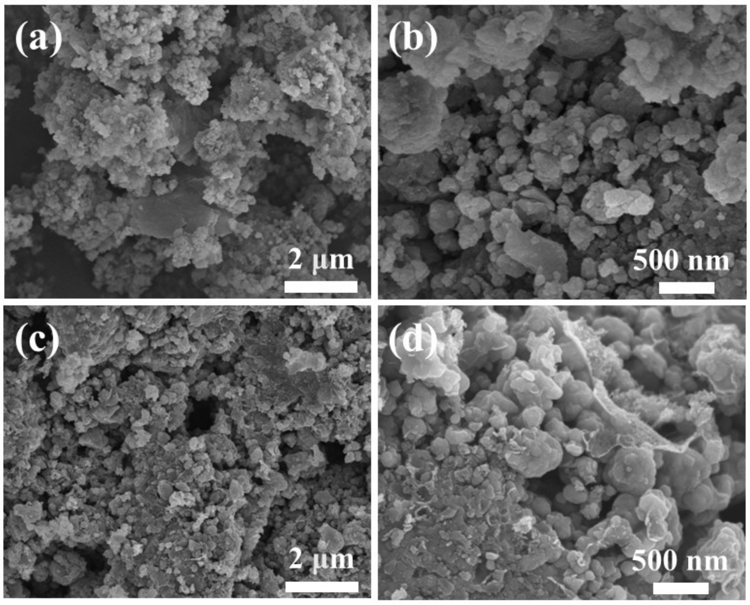

Figure S2. SEM images of (a-b) SiO-20/G, (c-d) SiO-20/G@TMA composite.

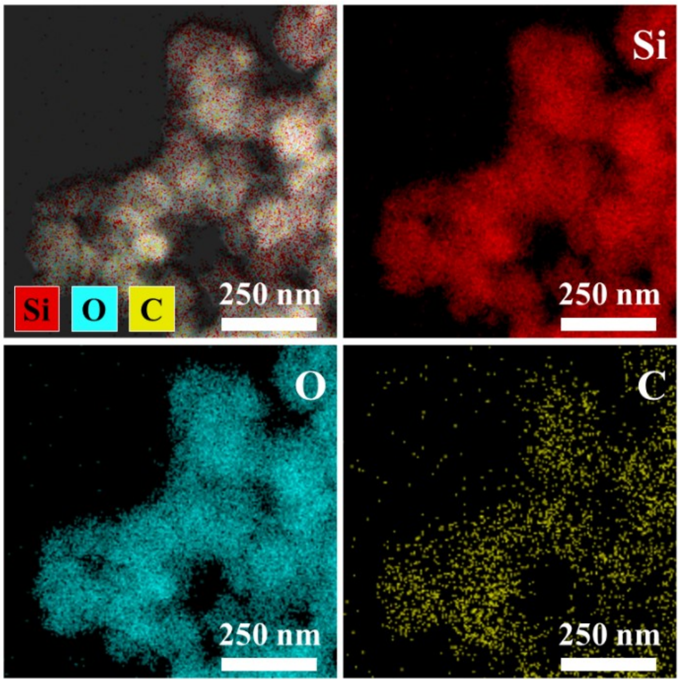

Figure S3. Mapping images of (a-c) SiO-20/G and (d-f) SiO-20/G@TMA composite.

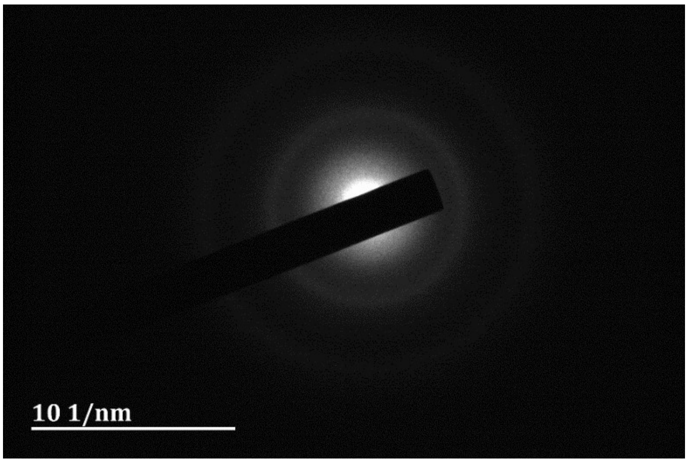

Figure S4. The selected area electron diffraction (SAED) pattern of SiO-20/G@TMA composite.

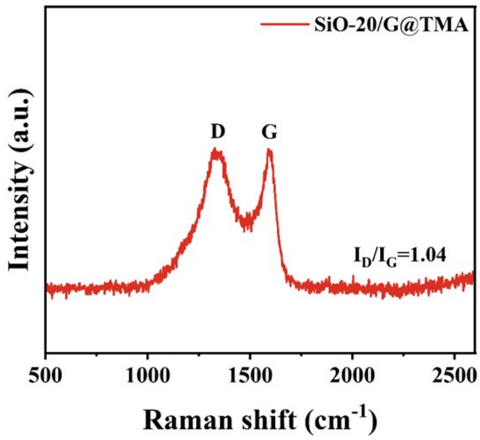

Figure S5. Raman spectra of SiO-20/G@TMA composite.

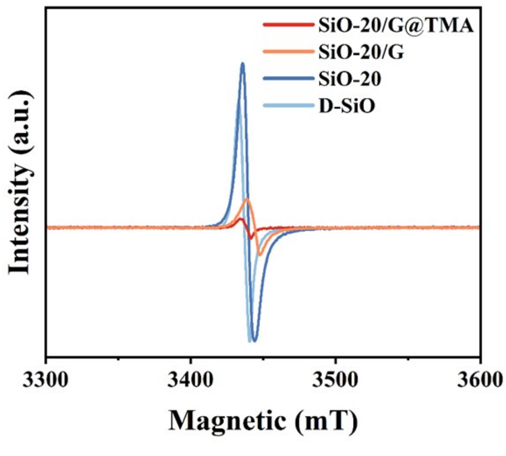

Figure S6. EPR patterns of the D-SiO, SiO-20, SiO-20/G and SiO-20/G@TMA composite.

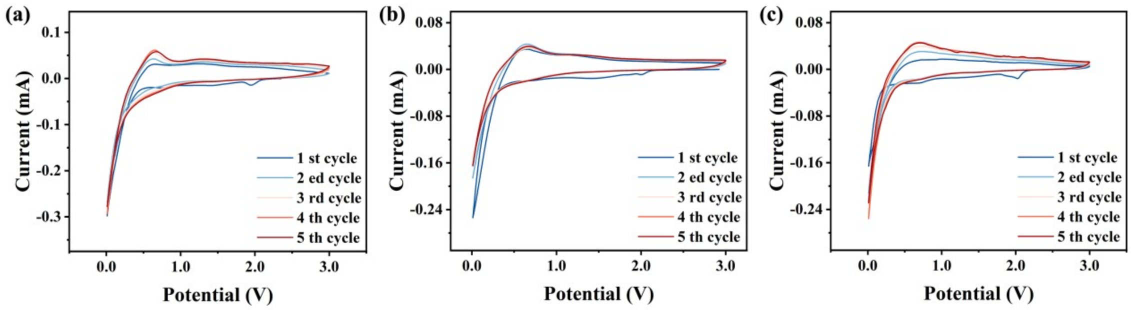

Figure S7. The CV curves of (a) D-SiO, (b) SiO-20, and (c)SiO-20/G at 0.1 mV s^{-1}.

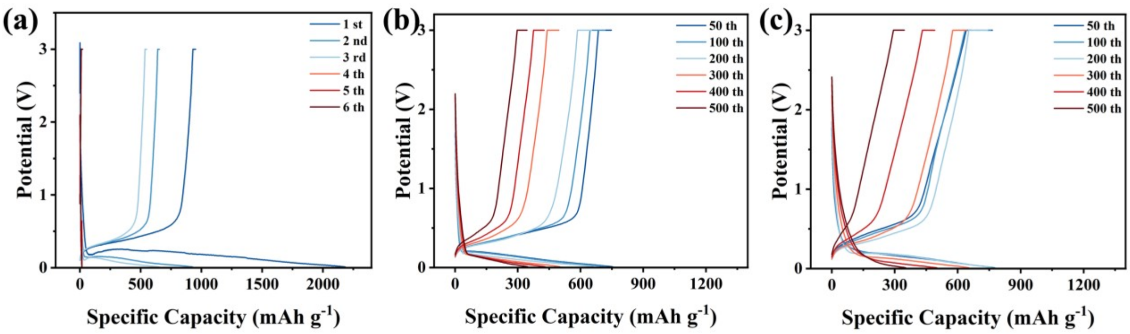

Figure S8. The galvanostatic charge/discharge curves at 0.5 A g^{-1} for (a) D-SiO, SiO-20 (b) and SiO-20/G, respectively.

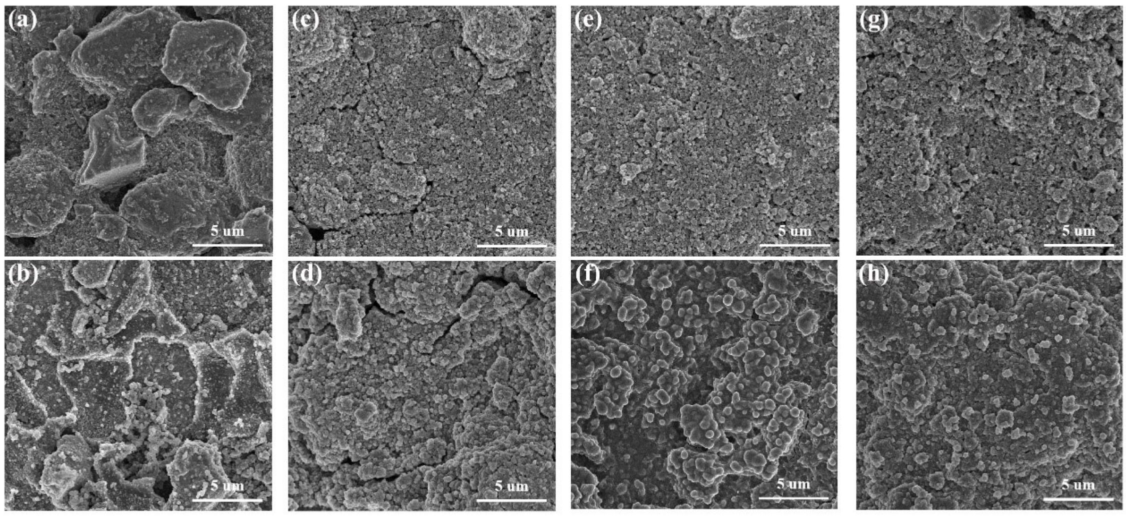

Figure S9. SEM images of the electrode plane for cycling (before, after) of (i, m) D-SiO, (j, n) SiO-20, (k, o) SiO-20/G and (l, p) SiO-20/G@TMA composite, respectively.

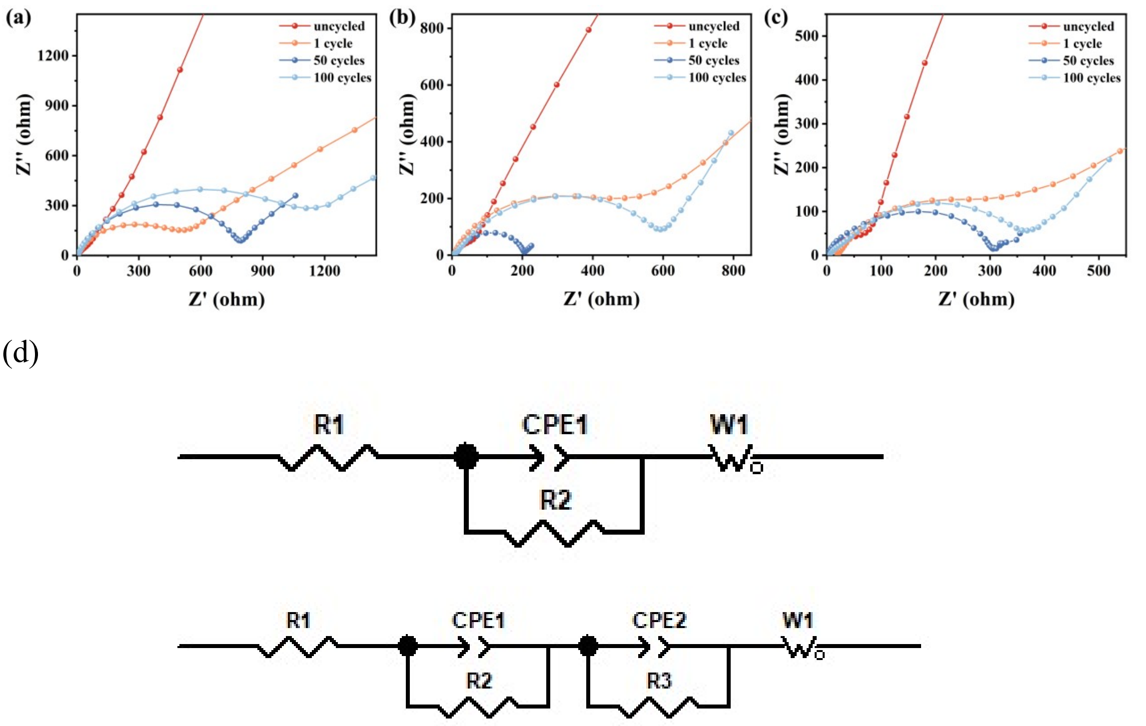

Figure S10. EIS plots of (a) D-SiO, (b) SiO-20, (c) SiO-20/G with different number of cycles and (d) equivalent circuit model.

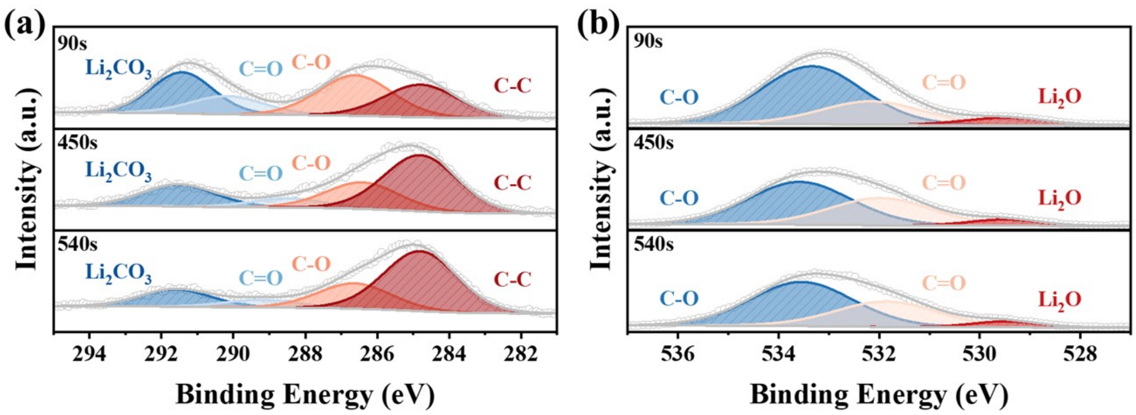

Figure S11. (a) C 1s and (b) O 1s spectra after 100 cycles of SiO-20/G@TMA electrode.

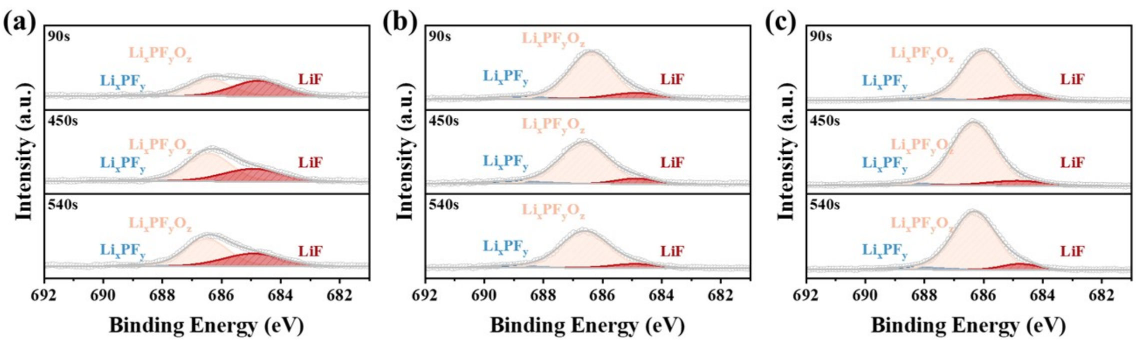

Figure S12. F 1s spectra of (a) SiO-20/G, (b)SiO-20 and (c) D-SiO after 90s, 450s and 540 s of Ar^{+} sputtering.

Table S1 The XPS integral area ratio of Si oxidation states in the Si 2p spectrum of each sample

Sample	Si^{4+} (%)	Si^{3+} (%)	Si^{2+} (%)	Si^{+} (%)	Si (%)
D-SiO	15.75	32.18	24.68	6.96	20.44
SiO-20	19.28	27.32	26.40	10.28	16.72
SiO-20/G	25.19	34.34	27.92	9.85	2.70
SiO-20/G@TMA	25.37	35.82	29.76	6.63	2.41

Table S2 Comparison of properties of SiO-20/G@TMA and reported SiO matrix composites

Sample	Current density ($A\ g^{-1}$)	Number of cycles	Specific capacity ($mAh\ g^{-1}$)	Reference
SiO_x/C	0.5	500	689.0	[1]
PSC	0.5	300	545.6	[2]
SiO_x/C/G	0.2	600	541.0	[3]
SiO/SG/C	3.0	300	442.0	[4]
SiO_x/C	0.1	100	600.0	[5]
SiO_x/C	0.1	250	510.0	[6]
Si@SiO_2@CNF	0.1	300	634.6	[7]
Si@C/CeO_2	0.1	180	502.2	[8]
N-doped C/SiO_x	0.6	200	488.0	[9]
SiO-20/G@TMA	0.5	600	649.1	This work

Table S3 Equivalent circuit fit values for different electrode materials before and after the cycle

Name	Before cycle	After cycle	
Samples	R_{ct} (ohm)	R_{SEI} (ohm)	R_{ct} (ohm)
D-SiO	153.90	92.28	755.20
SiO-20	108.80	31.12	63.36
SiO-20/G	95.32	15.32	54.21
SiO-20/G@TMA	53.81	8.42	40.99

References

[1] C.-M. Park, W. Choi, Y. Hwa, J.-H. Kim, G. Jeong, H.-J. Sohn, Characterizations and Electrochemical Behaviors of Disproportionated SiO and its Composite for Rechargeable Li-Ion Batteries, Journal of Materials Chemistry 20(23) (2010) 4854. https://doi.org/10.1039/b923926j.

[2] F. Song, X. Yang, S. Zhang, L.-L. Zhang, Z. Wen, High-Performance Phosphorus-Modified SiO/C Anode Material for Lithium Ion Batteries, Ceramics International 44(15) (2018) 18509-18515. https://doi.org/10.1016/j.ceramint.2018.07.071.

[3] Q. Xu, J.-K. Sun, G. Li, J.-Y. Li, Y.-X. Yin, Y.-G. Guo, Facile Synthesis of A SiO_x/Asphalt Membrane for High Performance Lithium-Ion Battery Anodes, Chemical Communications 53(89) (2017) 12080-12083. https://doi.org/10.1039/c7cc05816k.

[4] Y. Lu, Z. Zou, Y. Bai, X. Wang, H. Zhang, C. Jiang, Spent Graphite As Promising Carbon Matrix for High Performance SiO/C Anode Material of Li-Ion Battery, Journal of Energy Storage 72 (2023) 108711. https://doi.org/10.1016/j.est.2023.108711.

[5] Y. Ju, J.A. Tang, K. Zhu, Y. Meng, C. Wang, G. Chen, Y. Wei, Y. Gao, SiO_x/C Composite From Rice Husks As An Anode Material for Lithium-Ion Batteries, Electrochimica Acta 191 (2016) 411-416. https://doi.org/10.1016/j.electacta.2016.01.095.

[6] X. Gao, Y. Gao, Q. Li, Y. Wang, D. Zhao, G. Xu, Z. Zhong, F. Su, Scalable Synthesis of High-Performance Anode Material SiO_x/C for Lithium-Ion Batteries by Employing the Rochow Reaction Process, Journal of Alloys and Compounds 902 (2022) 163668. https://doi.org/10.1016/j.jallcom.2022.163668.

[7] X. Li, X. Wang, J. Li, G. Liu, D. Jia, Z. Ma, L. Zhang, Z. Peng, X. Zhu, High-Performance, Flexible, Binder-Free Silicon-Carbon Anode for Lithium Storage Applications, Electrochemistry Communications 137 (2022) 107257. https://doi.org/10.1016/j.elecom.2022.107257.

[8] J. Wang, Y. Mai, P. Yang, D. Guo, R. Sun, F. Wu, X. Dai, Y. Gu, H. Chen, Y. Cheng, Effect of Ce Incorporation into Carbon Layer on the Performance of Silicon-Carbon Composite As Anode for LIBs, Applied Surface Science 613 (2023) 156044. https://doi.org/10.1016/j.apsusc.2022.156044.

[9] H. Ma, C. Jin, G. Xu, L. Wen, C. Tu, F. Sun, Y. Li, L. Zhou, Z. Yue, High-Performance Free-Standing N-Doped C/SiO_x Film Anode Materials for Lithium Ion Batteries, Electrochimica Acta 471 (2023) 143402. https://doi.org/10.1016/j.electacta.2023.143402.